Th P5 15

Full-waveform Inversion of Surface Waves - Numerical Sensitivity Analysis

I. Silvestrov* (Institute of Petroleum Geology & Geophysics SB RAS), A. Bakulin (EXPEC ARC, Geophysics Technology, Saudi Aramco), M. Dmitriev (EXPEC ARC, Geophysics Technology, Saudi Aramco), K. Gadylshin (Institute of Petroleum Geology & Geophysics SB RAS), P. Golikov (EXPEC ARC, Geophysics Technology, Saudi Aramco), D. Neklyudov (Institute of Petroleum Geology & Geophysics SB RAS) & V. Tcheverda (Institute of Petroleum Geology & Geophysics SB RAS)

SUMMARY

We present the results of analysis of two full-waveform inversion formulations using surface waves. We explicitly construct the approximate Hessian matrix and study its properties using a truncated SVD approach. This analysis allows us to understand characteristics of the inversion algorithm such as the expected shape of the recovered solution, uncertainty of the results and the expected properties of local minimization algorithms being applied to this problem. This information should be useful for further development of the inversion strategy and for interpretation of the inversion results.

Introduction

Land seismic data generally contain strong surface waves propagating along the free surface. These waves are usually treated as noise in conventional data processing and special techniques such as receiver arrays and filtering are applied for their attenuation. However, surface waves contain valuable information about the near surface. In areas with challenging near-surface geology, images are often distorted by static shifts and waveform changes associated with the complex upper part of the subsurface. Therefore, attempts are made to use surface waves to derive static corrections or depth velocity model for migration from topography. These waves are dispersive in an inhomogeneous medium, and normally, dispersion curves are picked in frequency/phase-velocity panels to invert for a locally 1D S-wave velocity model (Socco and Strobbia, 2004). This approach is challenging to automate because of the need for picking. In addition, one may expect strong nonlinearity of the misfit function and limitations due to the 1D approximation. To address these issues a new approach, based on full-waveform fitting, was proposed for surface wave inversion (Pérez Solano, 2013; Massoni, 2013a,b; Pérez Solano, 2014). This new approach combines the standard full-waveform inversion technique (e.g. Virieux and Operto, 2009) with the dispersion curve analysis by inverting the misfit of amplitudes in the frequency/wavenumber domain between observed and synthetic data. It was shown that such a misfit function is more suitable for inversion of surface waves compared to the conventional full-waveform least-squares misfit in time or in frequency domains. In this study we continue the investigations of this modified full-waveform inversion approach and present numerical analyses of linear and non-linear inversion formulations based on singular value decomposition of the Hessian operator. This analysis allows us to understand the main features of the inversion algorithm such as expected shape of the recovered solution, uncertainty of the result and the expected properties of local minimization algorithms applied to this problem. This information should be useful for further development of the inversion strategy and for interpretation of the inversion results.

Theory

The classical least squares (CLS) misfit function can be written in the frequency/wavenumber domain as:

$$I_{CLS}(\mathbf{m}) = \left\| \hat{\mathbf{B}}(\mathbf{m}) - \hat{\mathbf{d}} \right\|^2, \tag{1}$$

where $\mathbf{m}$ is a model vector, $\mathbf{d}$ and $\mathbf{B}(\mathbf{m})$ stands for observed data and calculated data for the given model, and $\hat{\cdot}$ denotes a 2D Fourier transform in time and in space. The alternative misfit function proposed for inversion of surface waves has the form (Pérez Solano, 2013; Massoni, 2013a,b; Pérez Solano, 2014):

$$I_{FK}(\mathbf{m}) = \left\| \left| \hat{\mathbf{B}}(\mathbf{m}) \right| - \left| \hat{\mathbf{d}} \right| \right\|^2. \tag{2}$$

To handle lateral variations in the velocity model, Pérez Solano (2013) proposed a modification of equation (2) by first separating the data into subsets of consecutive receivers through spatial windowing in a similar fashion to what is done for standard dispersion curve inversion (Socco and Strobbia, 2004). In the current study, we will consider only a 1D inversion approach and will not use this modification. To minimize the misfit functions (1) and (2), the Gauss-Newton iterative algorithm can be used:

$$\mathbf{H}(\mathbf{m_{k+1}} - \mathbf{m_k}) = \nabla I, \tag{3}$$

where $\mathbf{m_k}$ is a model vector at the kth iteration, $\mathbf{H}$ is an approximate Hessian matrix and ∇I is the gradient of the misfit function. The approximate Hessian matrices and the gradients have the forms:

$$\nabla I_{CLS} = 2\Re\left(\mathbf{D}\hat{\mathbf{B}}^*(\hat{\mathbf{B}}(\mathbf{m}) - \hat{\mathbf{d}})\right), \quad \mathbf{H}_{CLS} = 2\Re(\mathbf{D}\hat{\mathbf{B}}^*\mathbf{D}\hat{\mathbf{B}})$$

$$\nabla I_{FK} = 2\Re\left(\mathbf{D}\hat{\mathbf{B}}^*\boldsymbol{\delta}\hat{\mathbf{u}}\right), \text{ where } (\boldsymbol{\delta}\hat{\mathbf{u}})_i = (\hat{\mathbf{B}}(\mathbf{m}))_i \frac{|(\hat{\mathbf{B}}(\mathbf{m}))_i| - |(\hat{\mathbf{d}})_i|}{|(\hat{\mathbf{B}}(\mathbf{m}))_i|}, \tag{4}$$

$$\mathbf{H}_{FK} = 2\mathbf{M}^{*}\mathbf{M}, \text{ where } (\mathbf{M})_{ij} = \frac{\Re\left((\mathbf{D}\hat{\mathbf{B}})_{ij}(\bar{\hat{\mathbf{B}}}(\mathbf{m}))_i\right)|(\hat{\mathbf{d}})_i|^{1/2}}{|(\hat{\mathbf{B}}(\mathbf{m}))_i|^{3/2}},$$

where $\mathbf{D}\hat{\mathbf{B}}$ is a Jacobian matrix, and $(\cdot)_i$ and $(\cdot)_{ij}$ denotes vector and matrix components. From equations (3) and (4) it is clear that each step of the non-linear inversion algorithm is governed by the linearized forward map $\mathbf{D}\hat{\mathbf{B}}$, and the Hessian determines, at least locally, convergence properties of the inversion algorithm. The exact inverse of matrix $\mathbf{H}$ usually cannot be constructed due to ill-conditioning and some regularization is needed. The truncated singular value decomposition allows to study properties of such regularized solutions (Assous and Collino, 1990; Cheverda et al., 1998; Silvestrov et al., 2013).

Numerical results

We consider in Figure 1 a 1D model similar to the one used in Massoni (2013a,b). The common-shot seismogram calculated in this model using 10Hz Ricker wavelet is shown in Figure 2, together with its 2D Fourier transform. The forward modeling $\hat{\mathbf{B}}(\mathbf{m})$ was performed in time domain by 2D elastic finite-differences with a free-surface boundary condition at the top of the model followed by 2D Fourier transform. To construct the Jacobian matrix $\mathbf{D}\hat{\mathbf{B}}$, we use the piecewise constant basis formed from 1D layers with thickness equal to 0.25m. The P wave velocity and density are kept constant and only an S wave velocity perturbation is considered. The matrix $\mathbf{D}\hat{\mathbf{B}}$ is constructed column by column using the following approximate relationship:

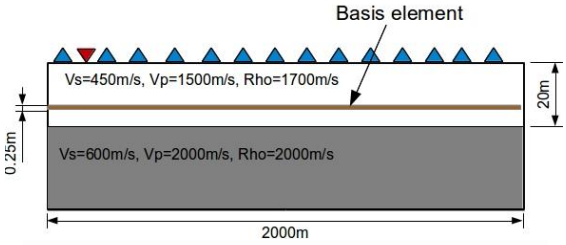

Figure 1 *The model used in the numerical experiments.*

$$(\mathbf{D}\hat{\mathbf{B}})_{ij} \approx \left[\left(\hat{\mathbf{B}}(\mathbf{m}+\varepsilon\mathbf{h}_j)\right)_i - \left(\hat{\mathbf{B}}(\mathbf{m})\right)_i\right]/\varepsilon,$$

where $\mathbf{h}_j$ is a j[th] basis vector, and ε is a small scalar value. Using the constructed matrix, $\mathbf{D}\hat{\mathbf{B}}$, the approximate Hessians $\mathbf{H}_{FK}$ and $\mathbf{H}_{CLS}$ are calculated. They have a similar shape, and we present only one of them (Figure 2). The columns of the Hessian matrix show the local sensitivity of the misfit with respect to perturbations of the basis elements. We see that this function is most sensitive at the very top and in the middle part of the first layer. The sensitivity to perturbations in the second layer are much less and are decreasing with depth. The normalized singular values and singular vectors of the matrices $\mathbf{H}_{FK}$ and $\mathbf{H}_{CLS}$ are shown in Figure 3. The singular values decrease rapidly and the first nine of them provide almost 10^6 condition number. It is unlikely, that we can achieve higher condition numbers when inverting noisy field data. The corresponding nine high-order singular vectors are relatively smooth inside the layers, and therefore we may expect the solution to be smooth as well. Figure 4 shows a projection of S-wave velocity perturbations onto the linear spans formed by these vectors in the two inversion formulations. The recovered solutions look similar in both cases, and therefore we can conclude that the two linear subspaces are close to each other. The solutions are smooth inside the layers and have variations around the correct S-wave velocity value. We may expect the same behavior in the non-linear formulation as well. This is illustrated in Figure 4, where the examples of non-linear inversion based on the conjugate-gradient method are shown. The inversion solution obtained using the $I_{FK}(\mathbf{m})$ function generally resembles the linear inversion results, thus showing that only few singular vectors are required in the non-linear case as well. The classical least-squares solution gets stuck in a local minimum in this example probably due to a poor initial model. The high-order singular vectors provide us the most sensitive directions of the misfit in multi-dimensional model space. Similar to Tompkins et al. (2011), we study the non-linearity of the problem along these directions by constructing 1D sections of the misfit function around the correct model:

$$f_i(\lambda) = I(\mathbf{m}_{true} + \lambda\mathbf{v}_i),$$

where $\mathbf{v}_i$ is the i[th] singular vector and λ is the scalar step length. The constructed functions are shown in Figure 5. We see that in all cases the modified misfit $I_{FK}(\mathbf{m})$ has wider valley of attraction than $I_{CLS}(\mathbf{m})$ and therefore is more suitable for minimization. The classic misfit function also has some local minima, especially for higher order vectors, which can adversely affect the minimization algorithm.

Conclusion

We present the analysis of two full-waveform inversion formulations applied to surface wave inversion. We explicitly construct the approximate Hessian matrix and study its properties using a truncated SVD approach. We show that a reliable solution is generally smooth and thus only a few smooth basis functions may be used in the inversion procedure. The singular vectors in both cases are similar, and we may expect the comparable inversion results when the initial model is close to the true one. However, when the initial model is further from the true solution, the modified misfit function has a more favorable shape for inversion using local minimization algorithms.

Acknowledgements

We acknowledge Saudi Aramco for support and permission to publish this work. The first author is also partially supported by RFBR (grants 14-05-31257, 14-05-00049, 15-55-20004, 15-35-20015).

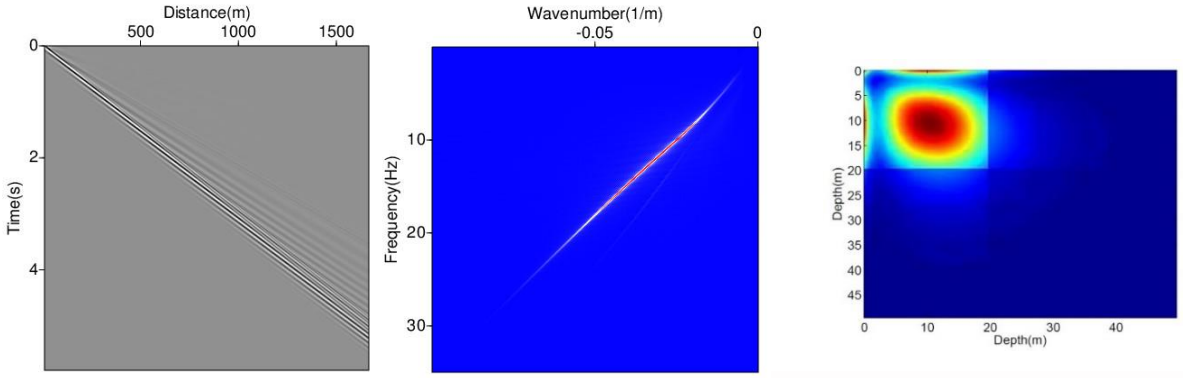

Figure 2 *Common-shot seismogram calculated in a 1D model (left) and its amplitude spectrum obtained by 2D Fourier transform (middle). Shape of Hessian matrix for* I_{FK} *misfit function (right). The shape for* I_{CLS} *is similar.*

References

Assous F. and Collino F. [1990] A numerical method for the explanation of sensitivity: The case of the identification of the 2D stratified elastic medium. *Inverse Problems* **6**(4), 487.

Cheverda V.A., Clement F., Khaidukov V.G. and Kostin V.I. [1998] Linearized inversion of data of multi-offset data for vertically inhomogeneous background. *Journal of Inverse and Ill-posed Problems* **6**(5), 453–484.

Masoni I., Valensi R., Brossier R., Virieux J., Boelle J.L., Leparoux D. & Cote P. [2013a] Toward a Better Full Waveform Inversion of Surface Waves. *Near Surface Geoscience*

Masoni, I., Brossier, R., Virieux, J. & Boelle, J.L. [2013b] Alternative misfit functions for FWI applied to surface waves, *in Proceedings of the 75th EAGE Conference & Exhibition incorporating SPE EUROPEC*, London, UK.

Pérez Solano C. A. [2013] Two-dimensional near-surface seismic imaging with surface waves: alternative methodology for waveform inversion. *Ph.D. Thesis.*

Pérez Solano C. A., Donno D. and Chauris H. [2014] Alternative waveform inversion for surface wave analysis in 2-D media. *Geophys. J. Int.*, **198**, 1359–1372.

Silvestrov, I., Neklyudov, D., Kostov, C. and Tcheverda, V. [2013] Full-waveform inversion for macro velocity model reconstruction in look-ahead offset vertical seismic profile: numerical singular value decomposition-based analysis. *Geophysical Prospecting*, **61**, 1099–1113.

Socco, L.V & Strobbia, C. [2004] Surface wave methods for near-surface characterisation: a tutorial, *Near Surface Geophys.*, **2**(2), 165–185.

Tompkins, M.J., Fernández Martínez, J.L., Alumbaugh, D.L., and Mukerji, T. [2011] Scalable uncertainty estimation for nonlinear inverse problems using parameter reduction, constraint mapping, and geometric sampling: marine controlled-source. *Geophysics*, **76**, (4), 263–281.

Virieux, J. & Operto, S. [2009] An overview of full-waveform inversion in exploration 1) geophysics. *Geophysics*, **74**, WCC1–WCC26.

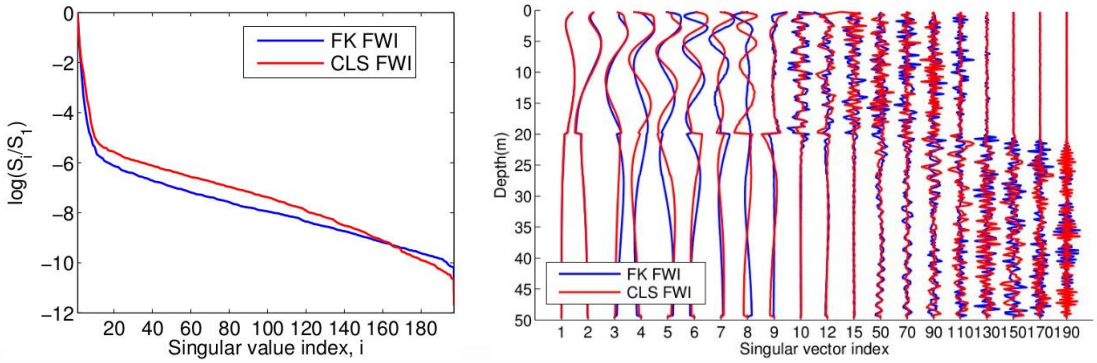

Figure 3 *Normalized singular values of the approximate Hessian matrices (left) and the corresponding singular vectors (right).*

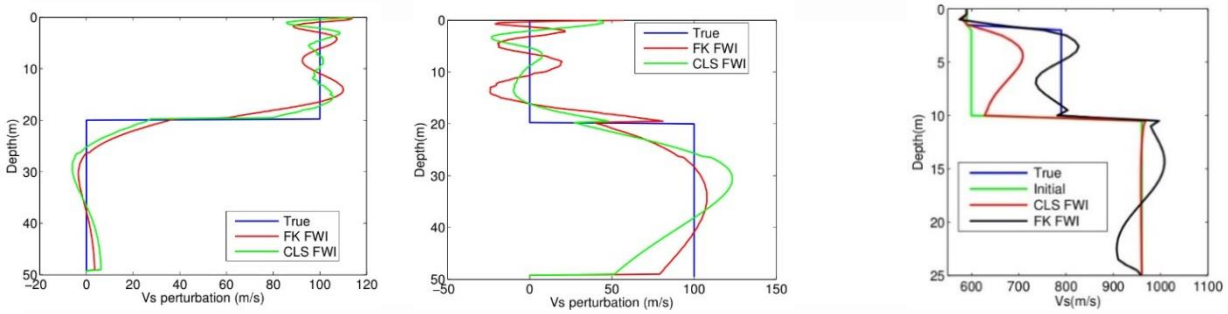

Figure 4 *Projections of S velocity perturbations onto a linear span of 9 high-order singular vectors (left and middle) and an example of the result obtained using non-linear full-waveform inversion based on a conjugate-gradient algorithm (right). Note that FK FWI delivers result closer to the true model, whereas classical FWI gets stuck in a local minimum.*

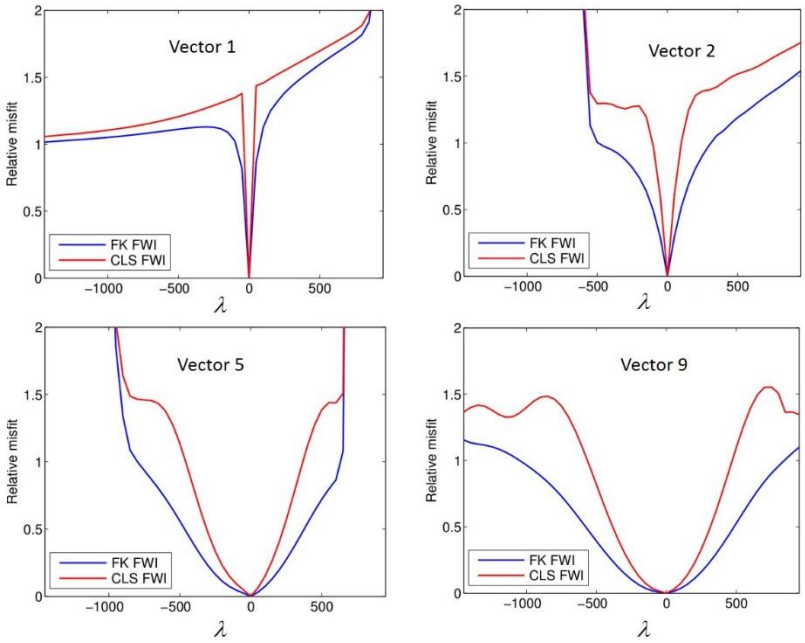

Figure 5 *Sections* $f_i(\lambda)$ *of the non-linear misfit functions along high-order singular vectors of the Hessian matrix.*